PAGEOPH, Vol. 121, No. 3, 1983 0033-4553/83/030443-33$1.50 + 0.20/0

Constitutive Relations for Fault Slip and Earthquake Instabilities

JAMES R. RICE[1]

Abstract - Constitutive relations for fault slip are described and adopted as a basis for analyzing slip motion and its instability in the form of earthquakes on crustal faults. The constitutive relations discussed include simple rate-independent slip-weakening models, in which shear strength degrades with ongoing slip to a residual frictional strength, and also more realistic but as yet less extensively applied slip-rate and surface-state-dependent relations. For the latter the state of the surface is characterized by one or more variables that evolve with ongoing slip, seeking values consistent with the current slip rate. Models of crustal faults range from simple, single-degree-of-freedom spring-slider systems to more complex continuous systems that incorporate nonuniform slip and locked patches on faults of depth-dependent constitutive properties within elastic lithospheric plates that may be coupled to a viscoelastic asthenosphere.

Most progress for the rate and state-dependent constitutive relations is at present limited to single-degree-of-freedom systems. Results for stable and unstable slip with the various constitutive models are summarized. Instability conditions are compared for spatially uniform versus nonuniform slip, including the elastic–brittle crack limit of the nonuniform mode. Inferences of constitutive and fracture parameters are discussed, based on earthquake data for large ruptures that begin with slip at depth, concentrating stress on locked regions within a brittle upper crust. Results of nonlinear stability theory, including regimes of complex sustained stress and slip rate oscillations, are outlined for rate and state-dependent constitutive relations, and the manner in which these allow phenomena like time-dependent failure, restrengthening in nearly stationary contact, and weakening in rapidly accelerated slip, is discussed.

Key words: Earthquakes; Fault mechanics; Friction.

Introduction

This paper reviews fault instability modeling. Throughout, tectonic shear faults are modeled as planar surfaces of (slip) displacement discontinuity in elastic surroundings. The relation of slip motion and its stability to the constitutive equations that describe slip on the fault surface is given particular attention. These constitutive equations relate shear strength τ along the fault to slip δ (Figure 1) and to other parameters such as normal stress σ_n,

[1] Division of Applied Sciences, Harvard University, Cambridge, Massachusetts 02138, USA.

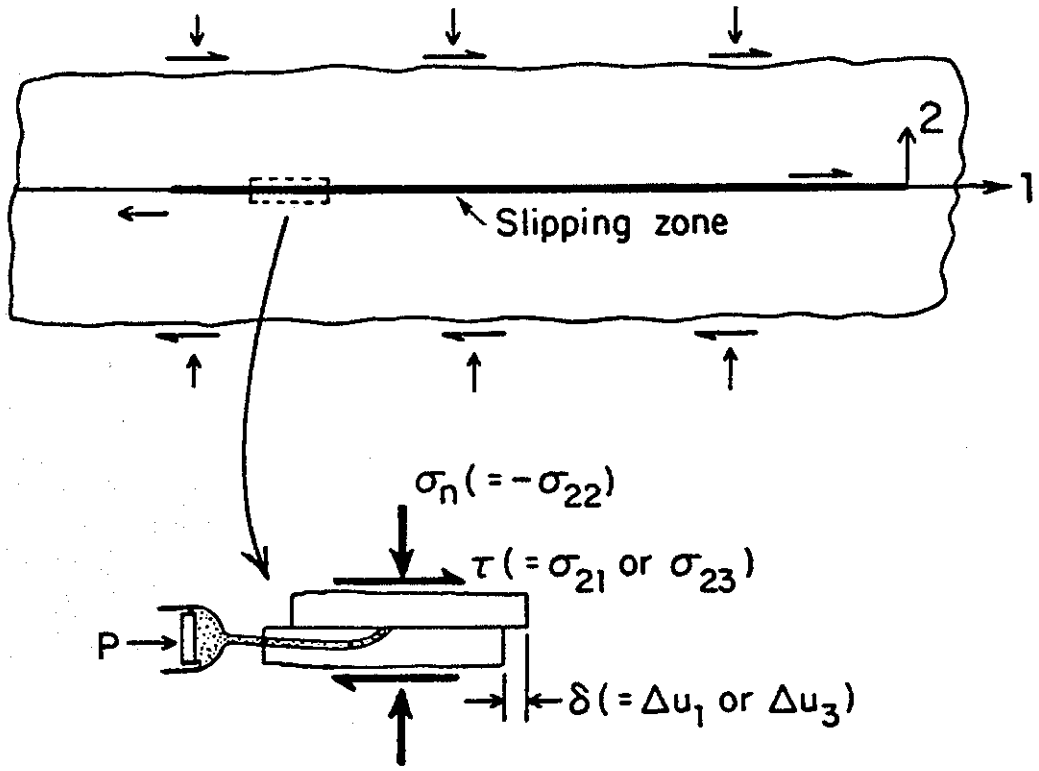

Figure 1. Section of fault modeled as a surface of possible slip displacement discontinuity. Notation: τ is shear stress; δ is slip displacement; σ_n is normal stress; p is pore pressure; σ_{ij} is the stress tensor; u_i is the displacement vector.

pore pressure p, temperature T, and rock and fault gouge mineralogy. Figure 1 shows a slipping region along a fault on the surface $x_2 = 0$ and shows how τ and σ_n are expressed by stresses σ_{ij}, and how δ is expressed by a discontinuity Δu_i of displacement u_i. According to whether slip is in the 1 or 3 direction, τ is identified as σ_{21} or σ_{23}, respectively. More generally, slip will occur in both directions and a complete constitutive description relates the pair σ_{21}, σ_{23} to Δu_1, Δu_3 (e.g., DAY 1982), although attention is restricted here to unidirectional slip.

Constitutive models

In the following discussion two types of constitutive models are adopted. The first is appropriate for the one-time motion of a fault segment that has been effectively stationary in its recent geological past. This constitutive model is referred to as a "slip-weakening" model. It embodies the elementary requirement that in order for a fault segment to exhibit seismicity, its strength must degrade with ongoing slip. The model is most simply represented graphically, as shown in Figure 2. In the plot of τ versus δ (Figure 2a),

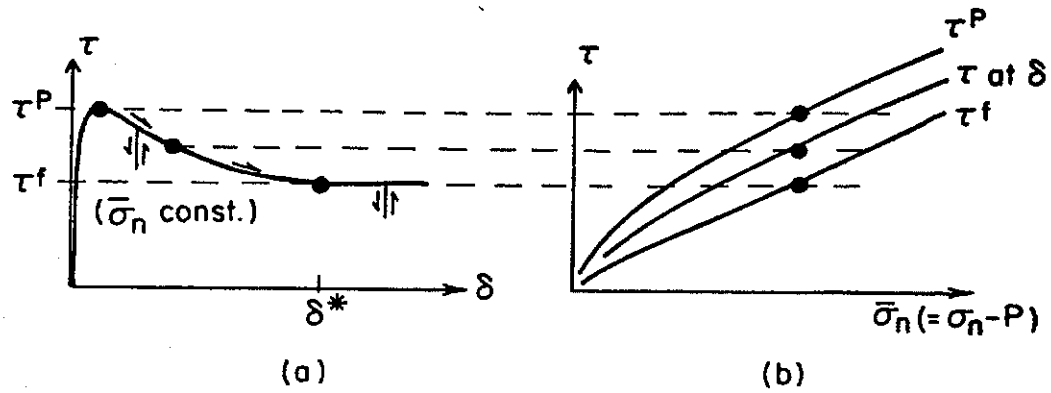

Figure 2. (a) Slip-weakening stress versus slip relations for constant effective normal stress; unloading and reloading branches shown. (b) Peak (τ^p), residual (τ^f), and intermediate strengths depend on effective normal stress, and also on temperature.

strength degrades in the slip δ^* from a peak resistance τ^p to initiate slip down to a fixed residual frictional level τ^f, where τ^f is sustained for larger amounts of slip. Response is of the rigid-plastic type, in that unloading and reloading occur along the vertical line segment shown. The plot in Fig. 2a envisions constant σ_n and p; if these change, τ^p, τ^f, and τ at any slip δ are altered, as shown in Figure 2b, where they are considered to depend on the effective normal stress $\bar{\sigma}_n = \sigma_n - p$.

The slip-weakening model has its roots in the well-known "cohesive zone" models of tensile fracture developed by Barenblatt, Dugdale, and Bilby–Cottrell–Swinden. The model was adapted to shear faulting by IDA (1972) and PALMER and RICE (1973), the latter including an account of residual friction τ_f at large slip; recently RICE (1980) and WONG (1982) have shown how slip-weakening τ versus δ relations for faults can be estimated from postpeak force versus deformation relations of laboratory triaxial specimens. The model as described is not explicitly rate-dependent and contains no provision for regaining strength with time after a slip episode, although some discussion has been presented of the effect of stress corrosion microcracking in causing a slip-rate-dependent τ versus δ relation for initially coherent rock (RICE, 1984).

Presumably, the difference between τ^p and τ^f, which describes the capacity for generating relatively sudden strength drops, should be assumed to decrease with increasing temperature and to first increase but then decrease with increasing $\bar{\sigma}_n$, thus describing the transition from cataclastic, or brittle, to ductile rock deformation. Since $\bar{\sigma}_n$ and T both generally increase with depth, the difference $\tau^p - \tau^f$ should firts increase and then diminish with greater depth. The brittle zone of high $\tau^p - \tau^f$ thereby defined models the "seismogenic" layer of the Earth's crust. Along the San Andreas fault in California, which is of transfrom or strike–slip type, this seismogenic layer ranges from 2 to 3 down to 10 to 15 km. The depths are greater in subduction

zones, presumably because the cold subducting plate depresses local geotherms. Applications of the slip-weakening and related concepts at a large crustal scale (STUART, 1979a,b; STUART and MAVKO, 1979; LI and RICE, 1983a,b) assume therefore that $\tau^p - \tau^f$ achieves a peak value in the seismogenic layer at a depth on the order of 10 km for transform fault condition and diminishes toward zero at greater depth.

The slip-weakening constitutive model as just outlined is plainly limited to description of a single fault slip sequence. Indeed, a feature of a more general constitutive relation, intended for description of sequences of repeated slip instabilities on the same fault surface, is that there can be no fundamental dependence of τ on δ. A general constitutive framework that meets this objection and is capable of incorporating dependences of strength on slip speed and prior slip history in a manner adequate to describe restrengthening has emerged in recent work by DIETERICH (1978, 1979a,b, 1981) and RUINA (1980, 1983). As commented by RICE and RUINA (1983), such constitutive relations as have been proposed fit a general framework in which stress $\tau(t)$ at time t at a point of a sliding fault surface is a direct function of slip speed $V(t)$ [$= d\delta/dt$] and $\bar{\sigma}_n(t)$ at that point and is a memory functional of the prior values $V(t')$ and $\bar{\sigma}_n(t')$ on the interval $-\infty < t' < t$. The necessity for such a memory dependence on $V(t')$ was noted much earlier by RABINOWICZ (1958) in an insightful discussion of the inadequacies of classical friction concepts.

Presuming that the memory dependence can be represented suitably by the current numerical values of some set of parameters, which themselves evolve with onging slip, one may cast the constitutive equations in the general form (RUINA, 1980, 1983)

$$\begin{aligned} \tau &= F(V, \bar{\sigma}_n, \Psi_1, \Psi_2, \ldots, \Psi_n); \\ d\Psi_i/dt &= G_i(V, \bar{\sigma}_n, \Psi_1, \Psi_2, \ldots, \Psi_n), \qquad i = 1, 2, \ldots, n. \end{aligned} \tag{1}$$

Here the set of parameters $\Psi_1, \Psi_2, \ldots, \Psi_n$ are called *state variables.* It would be satisfying to relate them to the microphysics of the slip process, and DIETRICH (1978, 1979a) argued for constitutive relations in which the (single) state variable involved was related to an effective time of contact between currently mating asperities. Alternatively, the state variables may simply be identified phenomenologically as parameters that enable description of experimental results. The latter is the approach taken by RUINA (1980, 1983), who showed, for example, that experimental records dominated by two prominent strength decay events after a sudden change of imposed slip speed could be simulated by constitutive relations involving two state variables that had no identity other than that endowed by the specific version of equations (1) they satisfy.

Later we shall examine the slip motion and stability of simple elastic systems that slip in compliance with specific forms of these constitutive

relations. Some general constitutive features have emerged, however, from experimental results reported by a number of workers (see Gu *et al.*, 1984 for a recent summary). These features are best discussed with reference to Figure 3, where a schematic record of stress τ at the slip surface versus displacement δ is shown for slip at constant $\bar{\sigma}_n$, just before and after a suddenly imposed change in slip speed from a constant value V_1 to a new constant value $V_2 (> V_1)$. The features are:

(1) There is a sudden increase in τ at the time of the velocity change (experiments with $V_2 < V_1$ show a sudden decrease). The sudden change in V is not accompanied by a sudden change in the Ψs, according to the constitutive framework of equations (1), and we therefore interpret the sudden change in τ to occur at a fixed state, with

$$(\partial\tau/\partial V)_{\text{fixed state}} > 0, \quad \text{or} \quad \partial F(V, \bar{\sigma}_n, \Psi_1, \ldots, \Psi_n)/\partial V > 0. \tag{2}$$

(2) In slip at constant speed V, τ evolves toward a "steady-state" value dependent on that speed and denoted $\tau^{ss}(V, \bar{\sigma}_n)$. We interpret this as meaning that for fixed V (and $\bar{\sigma}_n$) the latter set of equations (1) has solutions such that each Ψ_i evolves toward a steady-state value $\Psi_i^{ss}(V, \bar{\sigma}_n)$ that satisfies $G_i = 0$ for $i = 1, 2, \ldots, n$. The steady-state strength is then given by

$$\tau^{ss} = \tau^{ss}(V, \bar{\sigma}_n) = F[V, \bar{\sigma}_n, \Psi_1^{ss}(V, \bar{\sigma}_n), \ldots, \Psi_n^{ss}(V, \bar{\sigma}_n)]. \tag{3}$$

It may, of course, be the case that a steady state exists as a well-founded concept for slips over a distance scale like that illustrated in the figure, but that for much longer slips, even at constant V, there is a systematic change in τ as the fault evolves structurally, thermally, or chemically. In that case it may be assumed that some of the state variables relax as discussed above to steady state values, but that others maintain a gradual evolution.

(3) Apparently, $\partial\tau^{ss}(V, \bar{\sigma}_n)/\partial V$ can be of either positive or negative sign (the latter is shown in Figure 3), depending on normal stress conditions and temperature for a given rock–gouge–rock combination. Negative values of

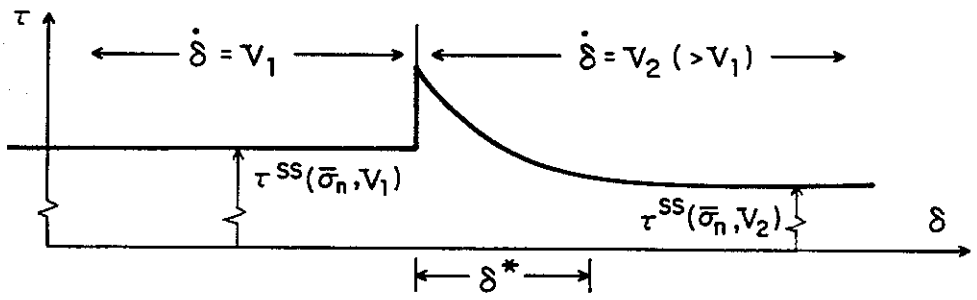

Figure 3. Rate and (evolving) state-dependent response to sudden increase of slip rate V at constant normal stress. Note the positive instantaneous viscosity, followed by evolution with ongoing slip toward a new strength level τ^{ss}, appropriate to the steady state at the new slip rate, which may be less or greater than the previous steady-state strength level. Velocity weakening is shown here.

$\partial\tau^{ss}/\partial V$ allow steady slip motions to become unstable to small perturbations, provided the effective elastic stiffness of the surroundings is low enough (RICE and RUINA, 1983). Thus the classical division of the normal stress and temperature plane into separate fields where either "stick–slip" or "stable sliding" resulted experimentally (BRACE and BYERLEE, 1970; BRACE, 1972) in the relatively soft testing machines of the time may be thought of as marking approximately the respective domains of negative and positive $\partial\tau^{ss}/\partial V$. Parameters that determine the positions of such domains in relation to mineralogy of the rock–gouge–rock system seem still to be rather incompletely understood (HIGGS, 1981), but increase of temperature seems generally to cause a transmission to stable sliding at the normal stress levels for which stick–slip occurs at lower temperature.

(4) Loss of memory of the prior slip history occurs over a characteristic amount of slip δ^*, Figure 3, which seems to be approximately independent of the magnitude of V. The decay of τ toward τ^{ss} in slip at fixed V is often modeled tolerably as the sum of one or two terms that have exponential decay with δ as measured from the inception of the slip at fixed V (DIETERICH, 1981; RUINA, 1980, 1983; GU *et al.*, 1984). There seem to be no published data on loss of memory of prior normal stress history. It is sometimes assumed that this loss is instantaneous, so that $\tau(t)$ is dependent on $\bar{\sigma}_n$ only through the current value $\bar{\sigma}_n(t)$; this is equivalent to a case for which the functions G_i of equations (1) are independent of $\bar{\sigma}_n$.

The rate and (evolving) state-dependencies of τ described here comprise an extremely small part of the total stress τ required to slip a fault, at least for variations by factors of, say 10^3 or less in V. In fact, these dependencies can be regarded as modest variations about a classically described critical τ for slip. This critical τ is given to a first approximation by the BYERLEE (1968) form

$$\tau = 0.85\,\bar{\sigma}_n, \quad \bar{\sigma}_n < 200\ MPa; \qquad \tau = 60\ MPa + 0.6\,\bar{\sigma}_n, \quad \bar{\sigma}_n > 200\ MPa \quad (4)$$

for a variety of rock types; clay gauges can exhibit substantially lower coefficients of $\bar{\sigma}_n$, of order 0.3 to 0.4, and there is very large scatter about the coefficient 0.85 at low $\bar{\sigma}_n$ when different rock types, surface roughness, etc. are considered. While the rate and state-dependent parts of τ are small compared to the total, they are nevertheless critical to understanding instability, because they embody the means by which strength can reduce in appropriate circumstances with ongoing slip, thus allowing seismic instabilities. Measures of rate sensitivity are given by

$$a = (V/\tau)(\partial\tau/\partial V)_{\text{fixed state}}, \qquad a - b = (V/\tau^{ss})(\partial\tau^{ss}/\partial V). \quad (5)$$

One finds that a and b are positive and of order of magnitude 0.01; as is clear from (3), $a - b$ may be positive or negative in different circumstances.

By comparing Figures 2a and 3 it becomes evident that rate and state-dependent frictional constitutive relations can sometimes lead to a response of a type that may be labeled "slip-weakening." This happens, particularly,

when a surface whose current state variables are comparable to those for steady slip at some speed V is suddenly obliged to slip at much greater speeds. This is what happens at the advancing edge of a zone of slip along a fault; OKUBO and DIETERICH (1981) observed τ and δ histories near the tips of propagating slip zones in a large rock friction apparatus with a slip-weakening appearance. It is perhaps less obvious that constitutive relations that describe response to sudden velocity jumps could also describe what could be called (in slip-weakening terminology) the time-dependent regain of peak strength τ^p after a rapid slip episode. Nevertheless, RUINA (1983) showed that his particular two-state-variable constitutive model closely described experimental results on time-dependent restrengthening in (nearly) stationary contact; it turns out to be critical to Ruina's explanation that very low-speed relaxational slips occur in what is nominally regarded as stationary contact.

While the rate and state-dependent constitutive framework just described with reference to equations (1) and Figure 3 is much more comprehensive than the rate-independent slip-weakening concepts of Figure 2, its richness is accompanied by complexity. Thus relatively little progress has been made up to the present on understanding consequences of the constitutive framework for instability with realistic fault models. In fact, at the present time a relatively complete understanding is in hand only for a severely simplified fault model, represented (Figure 4a) as a single-degree-of-freedom elastic system.

Slip-weakening fault instability models

The general description of fault instability, using rate-insensitive slip-weakening concepts, involves combining a constitutive description of the type illustrated in Figure 2 with the equations of elasticity for the surroundings and with a specification of the tectonic loading conditions. The result of the equations of elasticity is that there is a relation between the slip and stress distributions on a fault. Simplifying to undirectional slip, we have that the stress $\tau(P, t)$ at point P of the fault is related to slip $\delta(P', t)$ at points P' along the fault surface S, in a linear elastic medium, by an expression of the type

$$\tau(P, t) = \tau_0(P, t) - \int_S K(P, P')\delta(P', t)\, dS(P') \qquad (6)$$

under quasistatic conditions. Here $K(P, P')$ is an elastostatic Greens function, and what is written here as its integrated product with slip δ actually corresponds to the limit of a similar integral representation for general points P off the fault surface as P approaches a point on the fault. Also, $\tau_0(P, t)$ denotes the tectonic loading; for present purposes, we will regard the loading as specified. As is evident from equation (6), $\tau_0(P, t)$ is identifiable as the

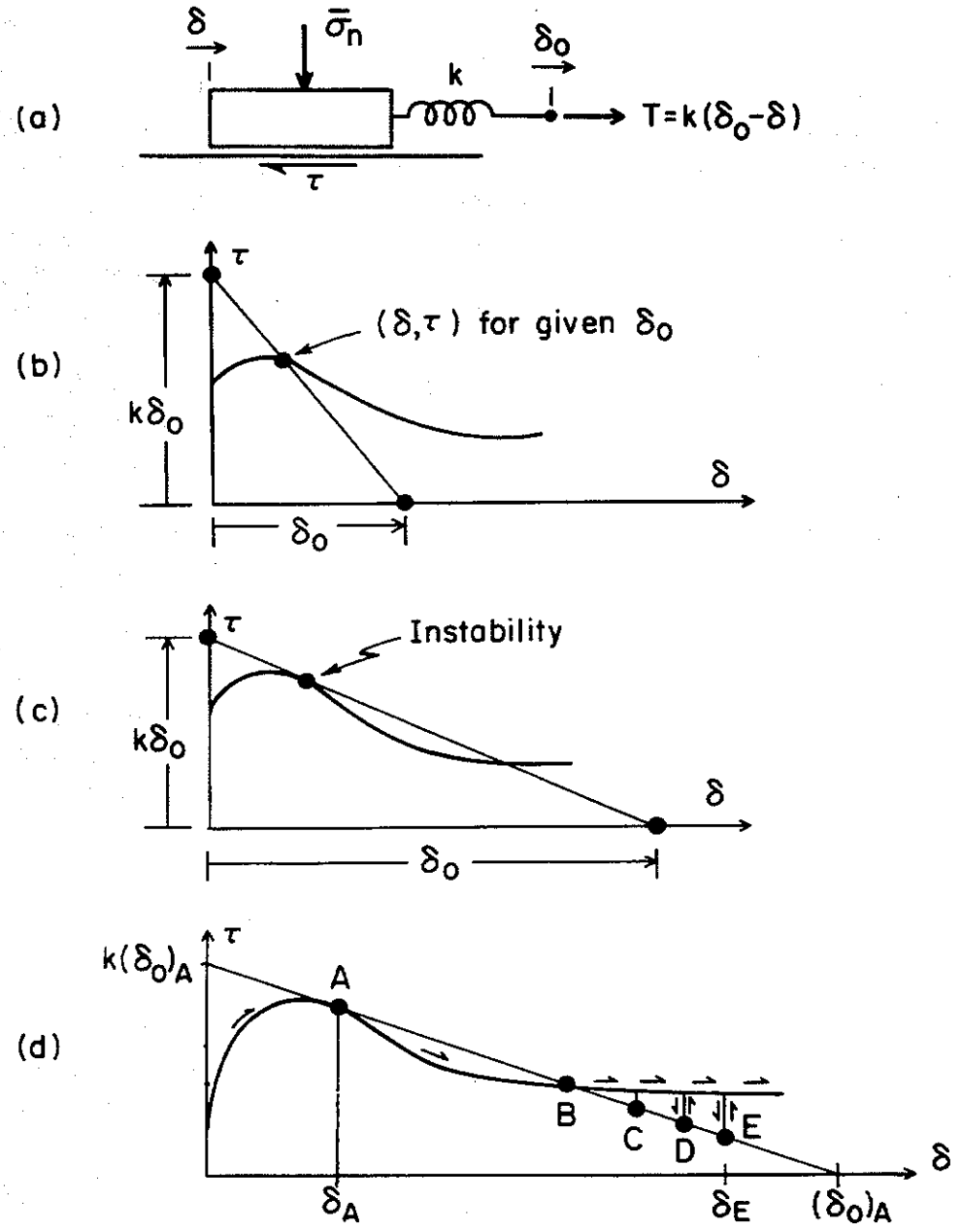

Figure 4. (a) Single-degree-of-freedom fault model. The block has unit base area. The spring is loaded by imposition of motion δ_0; $k\, d\delta_0/dt$ corresponds to the loading rate $d\tau_0/dt$, as discussed in the text. (b) Stable response of slip-weakening fault in stiff system. (c) Unstable response in soft system. (d) B, C, D, E denote possible final states after instability. If there is no radiated energy loss, the final state is E, for which the area under the straight line AE equals the area under the τ versus δ relation between δ_A and δ_E.

stress that would act at point P of a fault if the (entire) fault surface were constrained against slip offset.

The constitutive relation between τ and δ converts equations (6) to what may be regarded as a nonlinear integral equation for $\delta(P, t)$ with specified forcing function $\tau_0(P, t)$. Often, solutions $\delta(P, t)$ exist to this equation only up

to a finite limiting time, at which $\partial\delta(P, t)/\partial t \to \infty$ for some set of points P while $\partial\tau_0/\partial t$ is finite. This models a seismic instability, i.e., an earthquake. The actual dynamics of the instability are, at least in principle, described similarly, with equation (6) replaced by

$$\tau(P, t) = \tau_0(P, t) - \int^t \int_S \hat{K}(P, P', t - t')\delta(P', t')\, dS(P')\, dt', \tag{7}$$

using an elastodynamic Greens function $\hat{K}$.

Depending on constitutive and geometric details, the slip-weakening approach may lead to slip histories that are either entirely aseismic or terminated by seismic instability (STUART, 1979a; STUART and MAVKO, 1979) and involve extremes ranging from approximately uniform slip over a fault segment to strongly nonuniform slip in a crack-like mode. In the remainder of this section we examine the simple limiting extremes of essentially uniform and strongly nonuniform slip.

A faulted system that exhibits or is idealized as exhibiting spatially uniform slip and stress can be regarded as a single-degree-of-freedom elastic system in the form of a spring-loaded slider (Figure 4a) of unit base area. Equation (6) reduces in these circumstances to

$$\tau(t) = \tau_0(t) - k\delta(t) = k[\delta_0(t) - \delta(t)], \tag{8}$$

where k is an elastic stiffness in interaction with the surroundings. It is perhaps more natural to regard the loading of the slider as being specified by imposition of an imposed motion $\delta_0(t)$ of the spring end; hence we can write the second version of equation (8), for which it is seen that $\tau_0(t)$ has the interpretation $k\delta_0(t)$. Figures 4b and 4c illustrate the solution of the slip-weakening model under uncreasing imposed displacement δ_0. The state (δ, τ) that results for any given δ_0 is then the simultaneous solution of equation (8) and the slip-weakening constitutive relation. As is evident from Figure 4b, a succession of such states is traced out stably as δ_0 is increased in a system of sufficiently high stiffness k. This approximately models the aseismic slippage of a previously locked fault segment.

When the stiffness is too small, however, an instability as shown in Figure 4c, is encountered and this models the onset of a seismic slippage. The course of events after the instability may not be described adequately by the single-degree-of-freedom fault model, even if it provided an acceptable description prior to instability. Nevertheless, if a single-degree-of-freedom concept is adopted for the seismic motion, the final rest state of the system is constrained by the requirements that (1) the rest state must be a possible equilibrium state — i.e., it must satisfy the slip-weakening τ versus δ relation, possibly by lying along one of the rigid unloading branches (Figure 2a), and also equation (8) based on δ_0 at the onset of instability — and (2) the energy lost from the system, represented by radiated energy losses not explicitly included in the model of Figure 4a, must be nonnegative. The latter requirement means that the loss in spring energy cannot be less than the work done

on the friction surface:

$$\tfrac{1}{2}(\tau_A + \tau)(\delta - \delta_A) \geq \int_{\delta_A}^{\delta} \hat{\tau}(\delta')\, d\delta', \tag{9}$$

where $\hat{\tau}(\delta)$ denotes the τ versus δ relation for continuing slip, δ and τ denote the final rest state, and δ_A and τ_A denote the state at the instability. These requirements show that the final state must lie somewhere between points labeled B and E in Figure 4d. The upper limit point E corresponds to equality above—i.e., to an absence of radiated energy—and is chosen so that the area under the straight line AE is equal to that under $\tau = \hat{\tau}(\delta)$ between δ_A and δ_E.

The description of fault-slip and instability under the presumed conditions of uniform slip is probably a good description only of small laboratory specimens. As larger scales of size are considered, the slip-weakening process is predicted to become decidedly more nonuniform. This occurs because the constitutive relation contains a characteristic length scale (e.g., the slip distance δ^* in Figure 2), so that the usual concepts of scaling in continuum mechanics do not apply and the mode of failure in very large systems — i.e., with large size of the faulted region—is predicted to be so nonuniform that an elastic-brittle crack model of slip rupture applies as a limiting case.

The question of how large is "large" can be addressed within the model. Figure 5a shows schematic stress and slip distributions in the vicinity of the advancing tip of a long slipping region, advancing quasistatically into a previously locked fault segment. Local τ and δ values along the slipping section satisfy the slip-weakening relation $\tau = \hat{\tau}(\delta)$ illustrated in Figure 5b. The length ω of the zone of strength degradation at the slipping zone tip—i.e., the zone over which slips δ (which vanish at the tip) have not yet become large enough to reduce τ to its residual value τ^f—may be estimated approximately (RICE, 1980, eq. 6.12) as

$$\omega \approx [9\pi/16(1-\nu)]\mu\bar{\delta}/(\tau^p - \tau^f) \approx 2.4\mu\bar{\delta}/(\tau^p - \tau^f). \tag{10}$$

Here ν is the Poisson ration, μ the elastic shear modulus, and $\bar{\delta}$ is a characteristic displacement in the slip-weakening process defined by

$$\bar{\delta} = \frac{1}{\tau^p - \tau^f} \int_0^{\delta^*} [\hat{\tau}(\delta) - \tau^f]\, d\delta; \tag{11}$$

the integral represents the cross-hatched area in Figure 5b.

The length ω is what is desired for scaling. Slip-weakening on surfaces with dimensions much smaller than ω, e.g., in small through-cut laboratory specimens, can be assumed to involve uniform slip. As will be elaborated upon shortly, advancing slip regions with dimensions much larger than ω can (usually) be described well by calculations of elastic-brittle crack mechanics, which are relatively simple by comparison to the general formula-

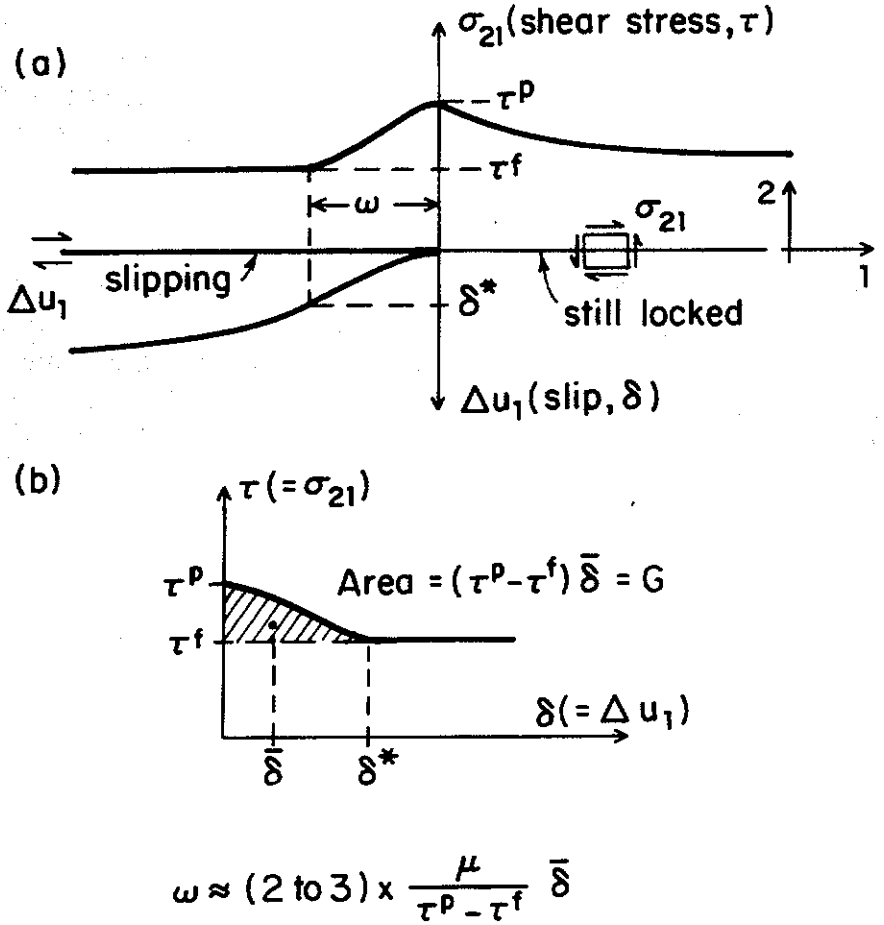

Figure 5. (a) Nonuniform stress along a fault as a slipping region advances into a locked section. (b) Slip-weakening relation followed between shear stress and slip. When zone ω, over which strength degradation occurs, is small compared to characteristic fault dimensions and to length scales associated with loading stresses the process may be described by elastic–brittle crack mechanics for fault-sustaining residual strength τ^f on slipping section, and supplying the fracture energy G, as indicated, for continued advance.

tion suggested in connection with equation (6). Of course, the middle ground for which ω and the size of the slipping region are more nearly comparable to one another requires a full implementation of the general formulation, which has actually been carried through in a few tectonically interesting cases (STUART, 1979a,b, STUART and MAVKO, 1979). The slip-weakening concept has also been applied to model the dynamics of rupture propagation (IDA, 1973; ANDREWS, 1976; BURRIDGE, *et al.*, 1979; DAY, 1982); this is not our present concern, but a recent review of studies on dynamic rupture is given by DMOWSKA and RICE (1984).

By extending the corresponding arguments for cohesive zone models of tensile cracks PALMER and RICE (1973) showed that the slip-weakening model led to predictions of conditions for crack advance that become indentical, in the limiting case $\omega \ll$ size of slipping region, to the following

elastic–brittle crack calculation: One neglects details of the slip-weakening process and assumes that all currently slipping regions of the fault surface sustain their residual frictional strength τ^f. Such a model leads to well-known singularities of the type (for Mode II, or in-plane slip, as in Figure 5a)

$$\sigma_{21} - \tau^f \to K_{II}/\sqrt{2\pi r} \tag{12}$$

at distance r along the fault plane ahead of the tip of the slipping region. Here K_{II} is the Mode II stress intensity factor. For Mode III, or antiplane slip, the relevant stress component is σ_{23} and the stress intensity factor is denoted as K_{III}; in general both modes may act simultaneously, but this tends to go beyond the present simplification to unidirectional slip. The energy drained through the crack tip singularity per unit area of fault over which the slip zone advances is

$$G = \frac{1-\nu}{2\mu} K_{II}^2 + \frac{1}{2\mu} K_{III}^2, \tag{13}$$

and the condition under which the slipping region can actually extend is that G as so calculated attain the critical value

$$G = \int_0^{\delta^*} [\hat{\tau}(\delta) - \tau^f]\, d\delta \equiv (\tau^p - \tau^f)\, \bar{\delta}, \tag{14}$$

represented as the cross-hatched area in Figure 5b.

Of course, the stress intensity factors have the form

$$K = (\text{numerical factor}) \times (\bar{\tau}_0 - \tau^f) \times \sqrt{\text{size}}, \tag{15}$$

where $\bar{\tau}_0$ is some appropriately weighted average of the loading stress that acts to slip the crack, being generally dependent on the "size" of the slipping region when the local loading stress τ_0 is nonuniform. Thus equation (13), with G set to its critical value in equation (14), provides an explicit criterion for how the loading stress must vary with the size of the slipping region to just maintain conditions for advance of that region into locked segments of the fault. It may happen, and usually does, that the following of this criterion ultimately requires the loading stress to diminish with advance of the slipping zone. Whether this process is stable or not may be judged by a stiffness-based analysis analogous to what is depicted in Figures 4b and 4c, as elaborated upon in LI and RICE (1983a,b), which is to be discussed further shortly.

Various estimates have been made of the parameters $\tau^p - \tau^f$, $\bar{\delta}$, ω, and G that enter this discussion. Based on an interpretation of the post-peak response in stiff servo-controlled laboratory triaxial tests of initially intact granite cylinders failing by shear fault formation while under confining stresses thought to be representative of seismogenic zones, RICE (1980) and WONG (1982) infer values for G in the range 5×10^3 to 5×10^4 J/m^2 and for $\bar{\delta}$ of the order 0.5 mm. The corresponding estimates of ω are of the order 0.5 to 1 m. It will be seen that these estimates for G, $\bar{\delta}$, and ω are far smaller than

what is inferred from crustal scale applications of slip-weakening and elastic–brittle crack models.

Crustal scale applications

Figure 6a shows the strike slip version of a widely adopted concept of how the brittle crust is stressed and ruptured in a great earthquake cycle. The dimension H represents the lithospheric thickness, and the lithosphere may be regarded as riding on a viscoelastic asthenosphere such that it is effectively decoupled in base shear from the asthenosphere during the slow rebuilding of tectonic stress in the period between great earthquakes. Of course, the coupling is significant in the coseismic and early postseismic stages, and probably also over periods of the order of one to several years prior to a great earthquake (LI and RICE, 1983b).

For the rupture modeling considered it is assumed that concentrated shear deformation takes place in the lithosphere, at the plate boundary considered. In the crustal depth regime this concentrated shear may be treated as slip along some megascale fault surface, to which slip-weakening and related fracture concepts may be applied. For the reasons mentioned earlier it is assumed that the strength drop $\tau^p - \tau^f$ associated with slip is relatively large in the seismogenic layer but falls off to negligible values at greater depths (and also decreases towards the Earth's surface, since $\bar{\sigma}_n$ is low there). Thus deeper regions along the plate boundary slip at effectively constant local stress $\tau = \tau^f \approx \tau^p$, whereas slip in the shallower regions occurs with a strength drop and hence can potentially result in an earthquake instability. Probably, the flow in the deeper regions of the lithosphere should be regarded as nonlinear viscous; the assumed flow at constant stress τ^f there is an approximation to this response.

At the end of an earthquake cycle the seismogenic layer has undergone a sharp drop in strength and thus carries a stress equal to τ^f, or possibly less if there is some dynamic overshoot (Figure 4d). Assuming that rehealing occurs (its reasons lie outside the present constitutive description), a much higher stress τ^p must be reached in that layer to reinitiate slip, and thus the seismogenic layer is effectively locked during much of the following earthquake cycle. Deeper portions of the lithosphere, however, underwent smaller or no strength drop in the previous earthquake. The stress there remains at or near a level appropriate for continuing slip, so that at a rather early stage in the next earthquake cycle a configuration like that in Figure 6a is expected to have developed. In that configuration ongoing tectonic loading causes slip to occur downdip from the seismogenic layer, but most of the layer itself is still understressed and locked. It is evident that stress concentration effects will occur at the upper border of the slipping zone, causing slip to be reinitiated locally there, and by this process the slipping region gradually penetrates upward into the effectively locked layer. Conditions are ulti-

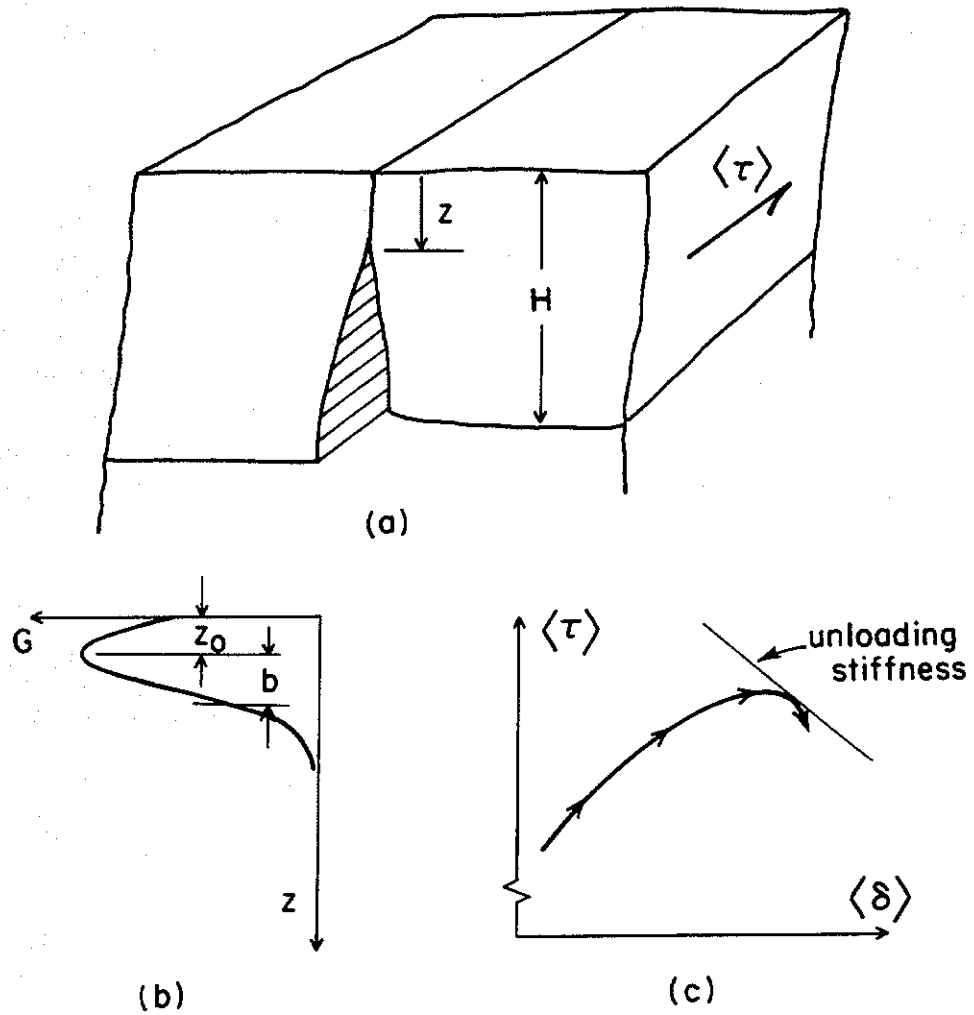

Figure 6. (a) Model of great earthquake instability in strike slip mode. Tectonic loading combined with slip or localized shear below concentrate stress on the locked upper crust; H is lithosphere thickness. (b) Fracture energy variations with depth for the elastic–brittle crack model of the advance of the slip zone. The peak of fracture energy simulates the brittle seismogenic layer. (c) Following Li and Rice (1983a,b), lithosphere-thickness-averaged stress $\langle \tau \rangle$ and slip $\langle \delta \rangle$ at the boundary are shown as crack advances to supply required fracture energy at the tip. In the simplest model instability occurs when the softening slope equals an effective elastic unloading stiffness (dependent on length along the strike and the mode of coupling to the asthenosphere) of fault surroundings, as in Figure 4b; more exact analysis includes viscoelastic coupling to the surroundings due to relaxation in the asthenosphere.

mately achieved such that this penetration process continues unstably and a great earthquake results. To the extent that this describes the earthquake cycle it is undoubedly affected by heterogeneities of strength and structure along strike. For example, a slipping region may partly surround and concentrate stress on a strong locked patch, sometimes called an asperity, and it has been suggested that certain precursory seismicity features can be understood in this way (Dmowska and Li, 1982). We first review simpler models,

which concentrate only on the effect of the depth dependence of properties and slip distributions.

STUART (1979a,b) and STUART and MAVKO (1979) have, in various studies, used a slip-weakening relation of the form

$$\tau - \tau^f = S \exp[-(z - z_0)^2/b^2]\exp(-\delta^2/\lambda^2), \tag{16}$$

where S, z_0, b, and λ are constant, and z denotes depth from the Earth's surface, to model depth variation of material properties. As employed by LI and RICE (1983a) in the elastic–brittle crack limit, this corresponds to a depth-dependent fracture energy G of the form

$$G = G_m \exp[-(z - z_0)^2/b^2]. \tag{17}$$

This is a Gaussian bell-shaped distribution with maximum value G_m at depth z_0 within the seismogenic layer and with variance width $b/\sqrt{2}$ (Figure 6b). When the upward progression of a slipping zone into the locked fault zone above it is considered, subject to the condition that the stress concentration at the tip of the slipping zone is sufficient to supply the requisite G as the tip progresses upward through each level z, there results a certain relation between thickness-averaged shear stress $\langle\tau\rangle$ in the lithospheric plate and the z to which the tip has advanced.One may then also calculate the thickness-averaged slip $\langle\delta\rangle$ at the plate boundary associated with each such pair of $\langle\tau\rangle$ and z values. Thus a $\langle\tau\rangle$ versus $\langle\delta\rangle$ relation may be defined for the boundary. This is shown in Figure 6c based on calculations by LI and RICE (1983a) for a G distribution as in equation (17). As one moves along the $\langle\tau\rangle$ versus $\langle\delta\rangle$ relation in the direction of the arrowheads shown, the tip of the slipping region moves progressively upward into the seismogenic layer. Ultimately a peak value of $\langle\tau\rangle$ is reached and further upward progression of the slipping zone occurs under decreasing stress. Similar relations between average stress and slip, exhibiting a peak and post-peak softening, have been shown by STUART (1979a,b) and STUART and MAVKO (1979) on the basis of the full slip-weakening formulation rather than just on its crack-like limit.

An elementary analysis of the seismic instability point in the process of upward progression of the rupture, analogous to that based on elastic spring stiffness for a single-degree-of-freedom slip model (Figure 4) is indicated by the line representing the elastic unloading stiffness of the surroundings in Figure 6c. The system becomes unstable when the softening slope $-d\langle\tau\rangle/d\langle\delta\rangle$ exceeds this stiffness. As analyzed by LI and RICE (1983a), the unloading stiffness at final instability is dependent on the along-strike length of the rupturing zone (see Figure 7), and also on the elastic properties of the asthenosphere, which becomes elastically coupled to the lithosphere in the terminal stages of pre-instability upward progression of the rupture, due to the rapid strain alterations that then occur.

In fact, the coupling to the asthenosphere is strongly time dependent. The fuller analysis of this viscoelastic coupling, by LI and RICE (1983a,b), sug-

gests that it may lead to an extended precursory period, of the order of a few months to several years, depending on parameters chosen within what they suggest as a representative range, during which deformation rates at the Earth's surface above the upselling rupture and stressing rates in the shallow crust are distinctly higher than those of previous decades in the earthquake cycle.

LI and RICE (1983a) emphasize the possible along-strike dependence of upward rupture progression and, following a procedure outlined by DMOWSKA and LI (1982), show how "line spring" concepts from tensile crack mechanics, developed originally for long surface cracks penetrating part-way through the wall of an elastic plate, can be adapted to deal with the problem. A representative along-strike variation in the great earthquake context is illustrated in Figure 7a, in the lithospheric cross-section of a plate boundary. The zone currently being driven toward instability is a slip-deficient patch along strike that remained locked while adjacent sectors slipped and were destressed in previous great ruptures. As shown in Figure 7b, the effect of the adjacent ruptures would be to concentrate the thickness-averaged stress $\langle \tau \rangle$ near the ends of the slip-deficient patch. This effect was

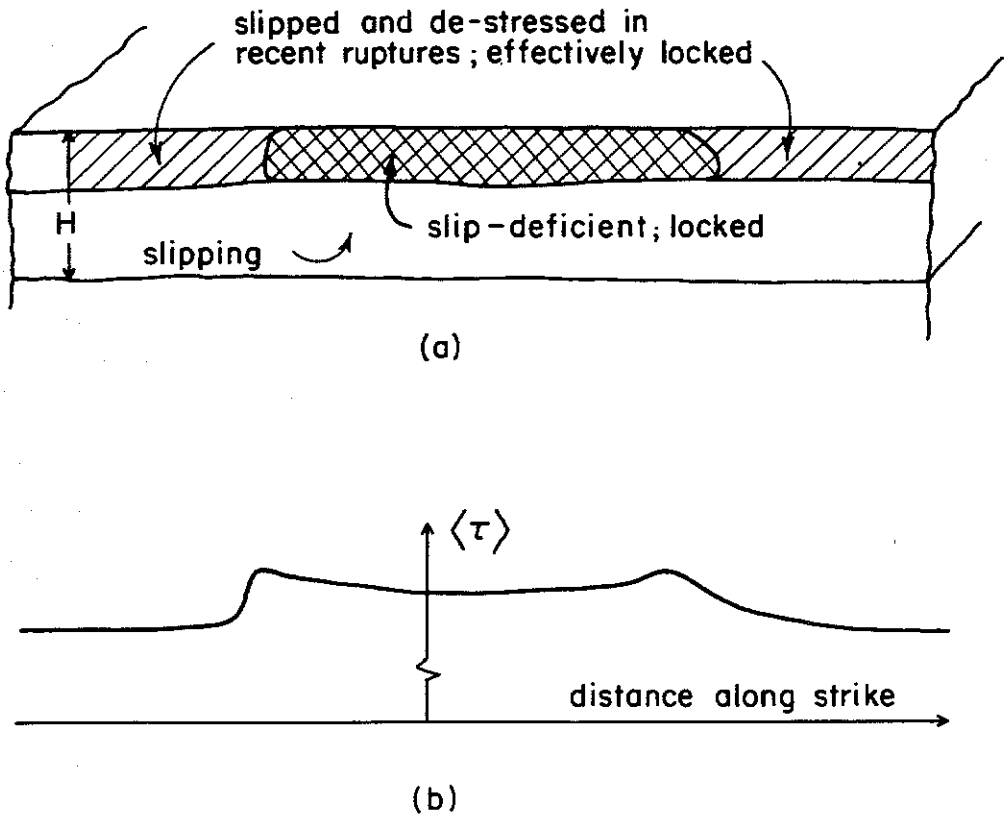

Figure 7. (a) Slip-deficient locked patch along strike, bordered by zones that have been relieved of stress by recent earthquakes. (b) Stress distribution concentrated near the ends of a locked patch.

neglected in the simple instability analysis of Li and Rice, who merely used an effective unloading stiffness appropriate to a finite zone along strike. As remarked by DMOWSKA and LI (1982), however, the real effect of such concentrations should be to cause preinstability seismicity to cluster at one or both ends of the slip-deficient gap and to cause the dynamic rupture not only to nucleate from below the slip-deficient gap, due to the upward progression of slip rupture, but to initiate toward one of the ends of the gap zone and propagate toward the other. As they point out, such features describe the accepted phenomenology of great earthquakes at plate margins (albeit based more abundantly on observations of margins of subduction rather than transform type) and lend confidence that the general framework for earthquake modeling is correct.

As regards the slip-weakening and fracture parameters associated with the large crustal-scale application discussed, LI and RICE (1938a) show that an assumed peak fracture energy G_m on the order of 4×10^6 J/m^2 is necessary to simulate the parameters of great strike-slip earthquakes within their modeling procedures. For example, calculations based on assumptions that such a peak occurs 7 to 8 km below ground surface and is the peak of a Gaussian bell-shaped distribution of G with depth, with variance on the order of 3 to 7 km simulating strength buildup in a seismogenic layer, leads to predictions of hypocentral depths slightly below the peak of G at 8 to 10 km and to nominal seismic stress drops of the order 40 bars and seismic slips of the order 2 to 4 m. The latter two parameters are proportional to $G_m^{\frac{1}{2}}$ for given depth to peak, bell variance width, lithospheric thickness, along-strike length, etc. and the 4×10^6 J/m^2 has been chosen accordingly; a G_m of 1×10^6 J/m^2 would reduce the nominal seismic stress drop and slips by a factor of one-half and may perhaps be considered equally plausible as a representative value.

As remarked by LI and RICE (1983a), the inferred range of G_m is consistent as to order of magnitude with independent seismic estimates for large earthquakes (IDA, 1973; RUDNICKI, 1980). It is also consistent with but a little larger than the corresponding values in the form $(\tau^p - \tau^f)\bar{\delta}$ used in the various crustal-scale simulations by Stuart (private communication, 1983).

In order to further constrain parameters for crustal-scale slip-weakening models (or their elastic–brittle crack limit), one may observe that as a slipping configuration like that in Figure 5a begins to propagate unstably in a manner generating detectable desimic signals, there is a distinctly nonuniform distribution of *stress drop* on the fault—i.e., of $\sigma_{12} - \tau^f$, where σ_{12} is the stress distribution as shown in Figure 5a evaluated just as the seismic event begins. The stress drop is equal to the *strength drop* $\tau^p - \tau^f$ at the tip of the preinstability slipping zone, but decreases to smaller values ahead of that zone, since σ_{12} diminished from τ^p and is equal to zero (at least for the present slip-rate-independent rupture model) along all portions of the preinstability slipping zone that slip further in the seismic event. Thus one must conclude

that $\tau^p - \tau^f$ is greater, perhaps by as much as a factor of 2, than stress drops extracted seismologically from rupture models that assume a uniform stress drop in the early stages of the seismic instability.

Such a uniform stress drop model has been developed by BOATWRIGHT (1980) based on fitting the average initial slope $\dot{u}_{peak}/t_{peak}$, up to the first peak in the seismologically recorded velocity record, to the intial slope of the theoretical Kostrov slip function for uniform stress drop on a circular rupture that extends from zero size at uniform speed. BOATWRIGHT (1984a,b) used this method to analyze eight moderate aftershocks of the Oroville, California, earthquake that occurred in a normal faulting environment over a 7 to 11 km depth range. He infers (BOATWRIGHT, 1984b) stress drops for the series ranging from 97 to 215 bars and averaging 158 bars. Assuming normal fault conditions and hydrostatic pore pressure, the limiting shear strength estimated (see the following) from Byerlee's relation, equation (4), ranges from 750 to 1190 bars over this depth range. Using 970 bars as an average, the nominal uniform dynamic stress drop is seen to amount approximately 16 percent of the Byerlee strength.

The suggestion that shallow earthquake stress drops correlate with estimates of the Byerlee strength is further supported by recent work by MCGARR (1984). He examines the parameter ρaR (where ρ is density, a is peak ground acceleration, and R is distance from source) for several normal and thrust earthquakes and finds that the parameter correlates within moderate scatter with the Byerlee strength as estimated at the focal depth for each event, and is of order 40% of that strength. For the case of the Kostrov growing circular rupture mentioned above, this parameter when based on body wave radiation is equal to the uniform stress drop times an orientation and directivity dependent factor of order unity, and times v^3/c^3 (v is rupture velocity, c is wave speed). Guided by the results discussed and by consideration of local stress concentration at the source, we may estimate $\tau^p - \tau^f$ very approximately as, say, 30 percent to 40 percent of the Byerlee strength.

The Byerlee equation is easy to apply for thrust and normal faults, because the overburden pressure ρgz (ρ = density of rock) at depth z can be assumed to be respectively, the minimum or maximum principal compressive stress. Figure 8 shows the "Mohr circle" implications, where the effective normal stress axis is labeled as $\rho gz - p$, and p is pore-water pressure at the location corresponding to the effective overburden pressure. If p is hydrostatic this effective overburden is $(\rho - \rho_w)\, gz$, where ρ_w is the density of water. The application of the Byerlee equation to vertical strike slip faults is not direct, because ρgz is then the intermediate principal stress. The circle labeled "strike slip" in Figure 8 takes the intermediate stress as the average of the other two principal stresses, but any circle between those for normal and thrust faults could apply.

For definiteness, let us consider seismic rupture nucleation at a depth of 8 km in a region of hydrostatic pore pressure. For $\rho/\rho_w = 2.9$ the Byerlee

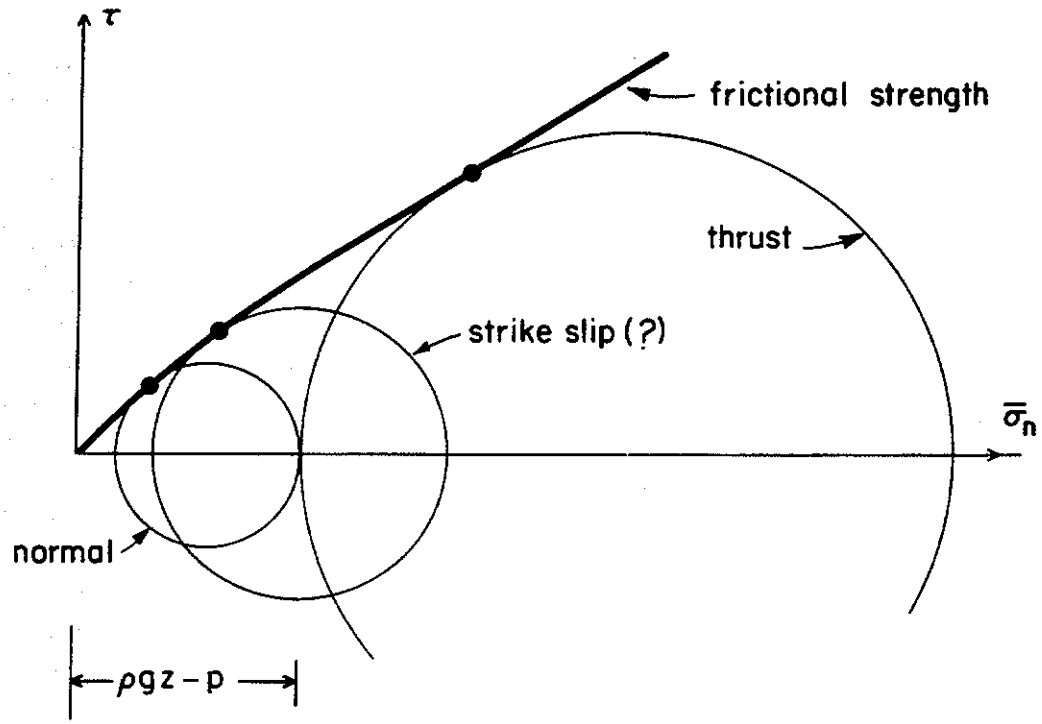

Figure 8. Limiting frictional strength, assuming that effective overburden pressure equals greatest (normal fault), least (thrust fault), or average (approximation for strike-slip fault) principal effective stress.

limiting strength is calculated from equation (4) by the procedure suggested in Figure 8. The Mohr circle centered on the effective overburden pressure touches the limiting friction line at a strength $\tau = 750$ bars; hence the estimate of $\tau^p - \tau^f$ is 200 to 300 bars. The estimate may vary from slightly smaller to much greater values, as is evident from the relative locations of the limiting τ for the normal and thrust limits to the strike slip geometry. Regrettably, for a given fracture energy G the characteristic weakening slip $\bar{\delta}$ and the size ω of the zone of strength degradation are strong functions of $\tau^p - \tau^f$,

$$\bar{\delta} = G/(\tau^p - \tau^f), \qquad \omega \approx 2.4\,\mu G/(\tau^p - \tau^f)^2, \tag{18}$$

so the uncertainty in $\tau^p - \tau^f$ prohibits tight constraints. Nevertheless, taking $\tau^p - \tau^f = 250$ bars (25 MPa), $G = 2 \times 10^6$ J/m^2, and $\mu = 30$ GPa as representative for a great strike slip earthquake nucleating at 8 km depth, one estimates $\bar{\delta} = 8$ cm and $\omega = 230$ m.

This result for ω is small enough compared to the large crustal scale considered that the elastic–brittle crack limit of the slip-weakening concept seems appropriate. However, there is considerable uncertainty, and it may be noted that a reduction by one-half of the inferred strength drop, which still represents a plausible case, would increase the estimated ω to 1 km. It does, however, seem that no plausible choices for G and $\bar{\delta}$ compatible with infer-

ences from seismology for large crustal earthquakes can be reconciled directly with the laboratory estimates of slip-weakening parameters discussed earlier, even though the estimated strength drops, $\tau^p - \tau^f$, are generally compatible with laboratory results.

The situation may arise because the laboratory results refer to slip on a well-defined fault surface, whereas what is modeled as a single planar fault surface on a large crustal scale may in fact consist of irregular segmented sections of fault, on the surfaces of each of which a laboratory-like description of slip-weakening applies, but which may be slipped cooperatively only by distributed inelastic rock deformation at the junctions between smaller misaligned fault segments. Such a picture is consistent with strengths and strength drops that are compatible with laboratory experience but with effective fracture ductilities, as measured by G or $\bar{\delta}$, that are much larger than those inferred in the laboratory for a single fault surface. The interpretation of the large G and $\bar{\delta}$ values just given also encourages the viewpoint that ω as estimated should be regarded as an approximate length scale of the region, near the tip of an advancing megascale slipping zone, over which individual misaligned fault segments are being reduced to their residual frictional strength level. It seems likely that this strength reduction could be accompanied by locally unstable events at the size scale of the individual segments, thus generating small-scale background seismicity even when the slipping zone as viewed at the crustal megascale is advancing quasistatically in the preinstability stage of the great earthquake cycle.

This concept relates to the suggestion of DMOWSKA and LI (1982) that seismicity patterns prior to great earthquakes may be related to the gradual upward progression of slip-rupturing regions into locked patches of plate boundary, and to the stress concentrations thereby induced (e.g., Figure 7). The present considerations suggest that a zone of a size related to what is estimated as ω, near the tip of the advancing megascale slipping region, may be a particularly fertile source of minor seismicity by comparison to deeper portions of the slipping region that are will slipped and to shallower portions of the fault zone that have not yet begun to slip. If such an idea is correct, improvements in the depth resolution of minor seismicity may serve to help track the upward progression of large-scale slip rupture in the preinstability period.

Rate and state dependent fault slip

As we have remarked, analysis of slip motion and stability for rate and state dependent and (evolving) state-dependent friction has not advanced much beyond the single-degree-of-freedom system in Figure 4a. The conclusions of the previous section also leave some uncertainty as to how understanding of slip on a single fault, modeled on laboratory studies, can be

extended to the large crustal scale. These factors notwithstanding, it does seem appropriate to review here some of the new viewpoints on slip motion and its stability that have emerged based on the more comprehensive rate and state-dependent constitutive framework. This is in the nature of a report on work in progress, since few definitive conclusions appropriate to fault motion as it occurs naturally as nonuniform slip on a fault have yet been drawn.

Linear stability analysis has been developed by RICE and RUINA (1983) for small departures from steady-state slip. The constitutive relation, when cast in memory-functional form and linearized about slip at steady velocity V_0, is

$$\tau = \tau^{ss} + f[V(t) - V_0] - \int_{-\infty}^{t} h(t - t')[V(t') - V_0]\, dt', \tag{19}$$

where τ^{ss} is the steady-state strength at speed V_0, $f = a\tau^{ss}/V_0$ (as defined in equation (5)), and $h(t) > 0$ represents the slope of the decay process in Figure 3, with $h(t) \geq 0$, $h(t) \to 0$ as $t \to \infty$, and

$$\int_0^{\infty} h(t)\, dt = b\tau^{ss}/V_0 \tag{20}$$

(b is as defined in equation (5)). Rice and Ruina analyze the single-degree-of-freedom system in Figure 4a, with mass m per unit contact area, constant normal stress, and imposed constant speed V_0 ($= d\delta_0/dt$) of the load point; i.e., equation (8) applies with $\delta_0(t) = V_0 t$ and the left side augmented by the inertia term $md^2\delta/dt^2$. Their result is that steady-state slip is always stable if $a > b$, i.e., if $\partial\tau^{ss}(V, \sigma_n)/\partial V > 0$. If $a < b$, i.e. $\partial\tau^{ss}(V, \sigma_n)/\partial V < 0$, such slip is found to go from stable to unstable by Hopf bifurcation as the stiffness k reduces below the critical value

$$k_{cr} = m\beta^2 + \beta \int_0^{\infty} h(t) \sin \beta t\, dt > 0, \tag{21}$$

where β is the circular frequency of oscillations at neutral stability (at stiffness $k = k_{cr}$) and is the unique (apart from sign) solution of

$$f = \int_0^{\infty} h(t) \cos \beta t\, dt. \tag{22}$$

Note that β depends on constitutive properties only, independent of mass m.

For example, in the case of a constitutive model of the type of equation (1) based on a *single* state variable Ψ (examples follow), $h(t)$ necessarily has the form

$$h(t) = (b\tau^{ss}/L) \exp(-V_0 t/L), \tag{23}$$

where L is a slip decay length (analogous to δ^* in Figure 3), and then the

frequency β and critical stiffness are

$$\beta = \frac{V_0}{L}\sqrt{\frac{b-a}{a}}, \quad k_{cr} = \frac{b-a}{L}(\tau^{ss} + mV_0^2/aL). \tag{24}$$

The last expression shows that steady state slip is stabilized by increases of stiffness and slip decay length, but is destabilized by increases of the steady-state velocity weakening $(b-a)\tau^{ss}$ and mass. When applied to steady slip between continuous elastic bodies (RICE and RUINA, 1983) a corresponding analysis shows that the response to perturbations of sufficiently short spatial wavelength is stable, but that to longer wavelengths may be unstable.

Results that extend beyond small perturbations from steady-state slip must be based on a full nonlinear form of the constitutive description. A procedure for constructing constitutive relations in the form of equations (1) from experimental measurements based on the a priori assumption (or approximation) that a *single* state variable Ψ suffices to characterize surface state is now outlined. For simplicity, assume σ_n = constant. The variable Ψ requires no a priori identification; it is assumed only to satisfy a set of equations of the form

$$\tau = F(V,\Psi), \qquad d\Psi/dt = G(V,\Psi). \tag{25}$$

Suppose that the variation of V with τ for rapid changes of stress, i.e., at fixed state, is observed. Such results can be summarized as a family of curves in the phase plane, whose axes are τ and V (RUINA, 1980, 1983). The curves can be regarded as the integral curves of the first of equations (5) with a given as $a(\tau,V)$, i.e., the integral curves of $d\tau/\tau = a(\tau, v)dV/V$. The state variable Ψ may now be introduced simply as a continuously variable labeling parameter for these curves, so that the curves of instantaneous response are equivalent to knowledge of a function $F(V, \Psi)$ such that

$$\tau = F(V, \Psi). \tag{26}$$

It is assumed further that the steady-state strength has been determined as $\tau = \tau^{ss}(V)$; such may be thought equivalent to specifying $a - b$ in the second of equations (5) and integrating with knowledge of τ^{ss} at some particular reference speed V_*. Finally, consistent what was discussed as item (4) earlier, the decay of τ toward $\tau^{ss}(V)$ in slip at constant V is fit to a single exponential decay with characteristic slip decay length presumed to be determined experimentally as $L = L(V)$. That is, $d\tau/d\delta = -(\tau - \tau^{ss})/L$ during slip at constant V, and setting $\tau = F(V, \Psi)$, $d\delta = V\,dt$, the relation

$$\frac{\partial F(V,\Psi)}{\partial \Psi}\frac{\partial \Psi}{dt} = -\frac{V}{L(V)}[F(V,\Psi) - \tau^{ss}(V)] \tag{27}$$

follows. However, this last equation expresses $d\Psi/dt$ as a function of Ψ and V and, although motivated by slip at constant V, it is immediately seen to be general, due to the a priori assumption that $d\Psi/dt$ is a function *only* of Ψ and V.

Consider the following two special cases of the above constitutive formalism:

(1) Assume a and b are constants in equations (5) and, consistently with an idealization of data mentioned earlier, L = constant. Then the constitutive relations are of the power-law form

$$\tau = \tau_* \Psi (V/V_*)^a, \quad \tau^{ss} = \tau_* (V/V_*)^{a-b}, \quad d\Psi/dt = -(V/L)[\Psi - (V/V_*)^{-b}]. \tag{28}$$

The state variable Ψ enters as a constant of integration for the first of equations (5), and here V_* is an arbitrarily chosen reference velocity at which the steady-state strength is τ_*; τ_* is dependent on σ_n.

(2) Following RUINA's (1980, 1983) simplification of a more complex law proposed by DIETERICH (1979a,b; 1980; 1981), suppose that $a\tau = A$ (constant) in the first of equations (5), and that $(a-b)\tau^{ss} = A - B$ (constant) in the second. This case is barely distinguishable from (1), since a and b are typically of the order 0.01, so that τ and τ^{ss} vary only modestly, even with substantial changes in V. The constitutive relations are then

$$\begin{aligned} &\tau = \tau_* + A \ln (V/V_*) + B\Psi, \quad \tau^{ss} = \tau_* + (A-B) \ln (V/V_*), \\ &d\Psi/dt = -(V/L)[\Psi + \ln (V/V_*)], \end{aligned} \tag{29}$$

where A and B are likewise to be regarded as functions of σ_n. This set of constitutive relations was originally proposed as a direct if approximate fit to experimental data. GU *et al.* (1984) discuss choices of τ_*/σ_n (about 0.6 for $V_* = 1\mu$m/s), A/σ_n, B/σ_n, and L to fit the data of DIETERICH (1981) for the sliding of intact Westerly granite on a gouge layer of the same material, with different layer thickness, gauge particle size, and degree of roughness of the intact rock faces. The latter is the most influential, and at $\sigma_n = 100$ bars for rough faces one finds $A/\sigma_n = 0.006$ to 0.008, $B/A = 1.12$ to 1.14, and $L = 40$ to 50 μm, whereas for smooth faces $A/\sigma_n = 0.003$ to 0.005, $B/A = 1.5$ to 2.3, and $L = 4$ to 25 μm.

It was found by RUINA (1980, 1983) that a somewhat better fit of his data on quartzite for stress decay toward steady state, following velocity jumps to a new constant slip speed, could be obtained by using a constitutive relation with two exponential decay processes with characteristic slip lengths L_1 and L_2 (0.3 and 5.2 μm in his case), but otherwise like that in equations (29). The relation is

$$\begin{aligned} &\tau = \tau_* + A \ln(V/V_*) + B_1\Psi_1 + B_2\Psi_2, \\ &d\Psi_i/dt = -(V/L_i)[\Psi_i + \ln(V/V_*)], \quad i = 1,2, \end{aligned} \tag{30}$$

where B_1 and B_2 are further constants, and

$$\tau^{ss} = \tau_* + (A - B_1 - B_2)(\ln)(V/V_*). \tag{31}$$

GU *et al.* (1984) discuss parameter choices in these constitutive relations to fit different experiments.

Some results of nonlinear analysis of slip motion and its stability

The linearized analysis of the stability of steady slip in response to imposed load point motion of uniform rate V_0, in the form summarized by equation (24) for one-state-variable constitutive laws applies, of course, to all laws of the type in equations (26), (27)—i.e., including those of equations (28), (29), provided that a and b are defined as in equation (5). The corresponding linearized results derived from equations (21), (22) for the critical stiffness and frequency at instability for the two-state-variable law of equations (30) are more lengthy, and are given by Gu *et al.* (1984). The latter authors also report results of nonlinear but quasistatic ($m = 0$) stability analysis for the one- and two-state-variable laws of logarithmic character in equations (29) and (30). For example, they find that for the two-state-variable law stable limit cycle oscillations of $V(t)$ about V_0 accompany the Hopf bifurcation for a range of k in a small neighborhood below k_{cr}. Remarkably, for the special choice of parameters reducing that law to the one-state-variable law of (29) this neighborhood collapses to the line $k = k_{cr}$, and sustained oscillations of any amplitude below a certain limit are possible with $k = k_{cr}$. At large amplitude, near the limit, these have the character of relaxation oscillations: $V(t)$ lags behind V_0 for much of the period, and stress builds up in the spring until a short burst of large $V(t)$ causes the block to surge ahead and the spring to unload, beginning the cycle again.

The situation can be summarized with reference to Figure 9, which shows the nature of the response found by Gu *et al.* (1984) for the following problem: A quasistatic single-degree-of-freedom system slides in steady state at speed V_0, and then the imposed speed at the load point is changed abruptly to $V_0 + \Delta V_0$. For the law (30) with choice of parameters making $d\tau^{ss}/dV < 0$ it is found that the response to small perturbations is of course stable, $V(t) \to V_0 + \Delta V_0$ with increasing time, for stiffness $k > k_{cr}$ of linear stability theory. However, sufficiently large perturbations with $k > k_{cr}$ always cause instability (Figure 9). These instabilities appear in the quasistatic analysis based on such constitutive laws as motions for which $V(t) \to \infty$ in finite time. They occur even though the system considered would be stable (to sufficiently small perturbations) when in steady slip at the altered speed $V_0 + \Delta V_0$; in this case k_{cr} is independent of V_0.

All perturbations with $k < k_{cr}$ produce some permanent alteration of the steady motion. As indicated in Figure 9, perturbations of any size when k is sufficiently reduced below k_{cr} cause instability, $V(t) \to \infty$ in finite time, although for a small range of k below k_{cr} and sufficiently limited magnitude of perturbation there result permanently sustained oscillations of $V(t)$ about V_0. These oscillations are the limit cycle oscillations of the Hopf bifurcation at k_{cr} when k is only slightly below k_{cr}, but Gu *et al.* (1984) find that the limit cycle oscillations become more complex with decreasing k, exhibiting period doubling and, with further decrease of k (but still within the region of sus-

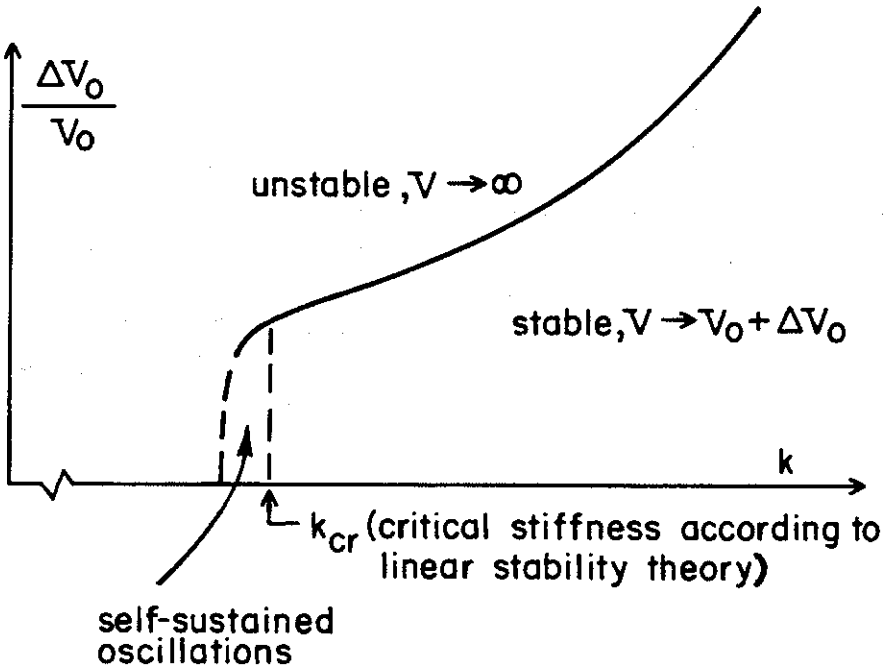

Figure 9. Effect of sudden change of imposed speed of load point, form V_0 to $V_0 + \Delta V_0$, based on quasistatic analysis of the spring-slider system (Figure 4a) originally in steady-state slip at speed V_0 and obeying the two-state-variable constitutive law of logarithmic character, equations (30).

tained oscillations), transition to apparently chaotic oscillations. The amplitude and shape of the limit cycle oscillations depend only on k and are independent of ΔV_0, provided that it lies in the domain indicated. Complex quasistatic oscillations with some features in common with such predictions have been observed (RUINA, 1980; GU *et al.*, 1984). For the special choice of parameters in (30) reducing the two-variable law to the one-variable law of (29) it is found that the region of sustained oscillations collapses to a vertical line extending above $k = k_{cr}$ to the limiting perturbation amplitude $\Delta V_0/V_0 = A/(B - A)$. In fact, the boundary separating unstable from stable response when $k > k_{cr}$ in Figure 9 is given approximately for the one-variable law of (29) by

$$\Delta V_0/V_0 \approx [A/(B - A)][1 - e + \exp(k/k_{cr})]. \tag{32}$$

The collapse of the region of sustained oscillations is apparently not common to all one-state-variable laws. DIETERICH (1980) shows such oscillations for a law only modestly different from (29).

A more comprehensive understanding of nonlinear stability for the one-state-variable law of (29) is provided by the work of GU *et al.* (1984) and some recent extensions of it by RICE and GU (1983). They consider quasistatic motions with uniform load point speed V_0, corresponding to uniform loading rate $\dot{\tau}_0 = kV_0$ in (8), although it is to be understood that a more

complicated loading process may have preceded the present uniform rate. It is found that all motions must be stable in the sense that $V(t) \to V_0$ as $t \to \infty$ if $d\tau^{ss}/dV > 0$—i.e., if $A > B$. Nevertheless, strong perturbations of the system (e.g., sudden displacement of the end of the spring, say, analogous to sudden stress loading of a fault segment due to a neighboring earthquake) can in certain circumstances lead to motions with large transient speeds, $V(t) \gg V_0$, even though the speed ultimately reduces and $V(t) \to V_0$. A spring-loaded system with $d\tau^{ss}/dV > 0$ may approximately model slip on downdip extensions of crustal faults below the seismogenic layer. For example, laboratory results of STESKY (1978) on Westerly granite suggest that a transition from $d\tau^{ss}/dV < 0$ to $d\tau^{ss}/dV > 0$ occurs as temperature rises, with increasing depth, above approximately 250 to 300°C. Thus such downdip extensions may slip with $d\tau^{ss}/dV > 0$, and when they are loaded suddenly by crustal earthquakes above there would then result transiently accelerated slip as a short-term response in the immediately postseismic regime of the earthquake cycle.

Evidently, faults of the brittle seismogenic crust are to be understood as exhibiting $d\tau^{ss}/dV < 0$—i.e., $B > A$ in the representation by (29). For such conditions it is found that all motions of the spring-loaded slider are unstable, in that $V(t) \to \infty$ in finite time, if k is less than k_{cr} of linear stability theory. Nevertheless, motions that begin with V much less than V_0 and τ much reduced from the steady-state strength $\tau^{ss}(V_0)$ may of course take a long time, longer than $(\tau^{ss} - \tau)/\dot{\tau}_0$, to reach instability. The characterization of motion changes dramatically when $k \geq k_{cr}$. For all such cases a "stability boundary" (RICE and GU, 1983) exists in a phase plane whose axes denote τ and V. Such is shown in Figure 10 for a few values of k for a case with $(B - A)/A = 0.6$. Each boundary separates the unstable region, $V(t) \to \infty$ in finite time, above it from the stable region, $V(t) \to V_0$, below it. The boundary is itself a possible trajectory of the system at the stiffness indicated. RICE and GU (1983) show how such diagrams can be used to analyze, within the spring–slider model, the response of fault segments to various perturbations. These represent, for example, sudden alterations of loading stress as appropriate for the analysis of aftershock phenomena, and also alterations of loading stress rate. The latter is predicted late in the preinstability period for some fault models. Altered stress rates may also result from accelerated deep lithospheric and asthenospheric readjustments, over perhaps one to a few tens of years after great earthquakes, that redistribute stress in the adjacent brittle crust.

The analysis of quasistatic motion for the spring–slider satisfying (29) simplifies considerably if the slip rate V is much greater than the load point rate V_0. Then one may set $V_0 = 0$, and in this case GU *et al.* (1984) show that the family of trajectories in a phase plane analogous to that of Figure 10 is given by

$$\exp(\lambda f/K)[f + \lambda \ln (V/V_*) - K(1 + \lambda)/\lambda] = \text{constant} \qquad (33)$$

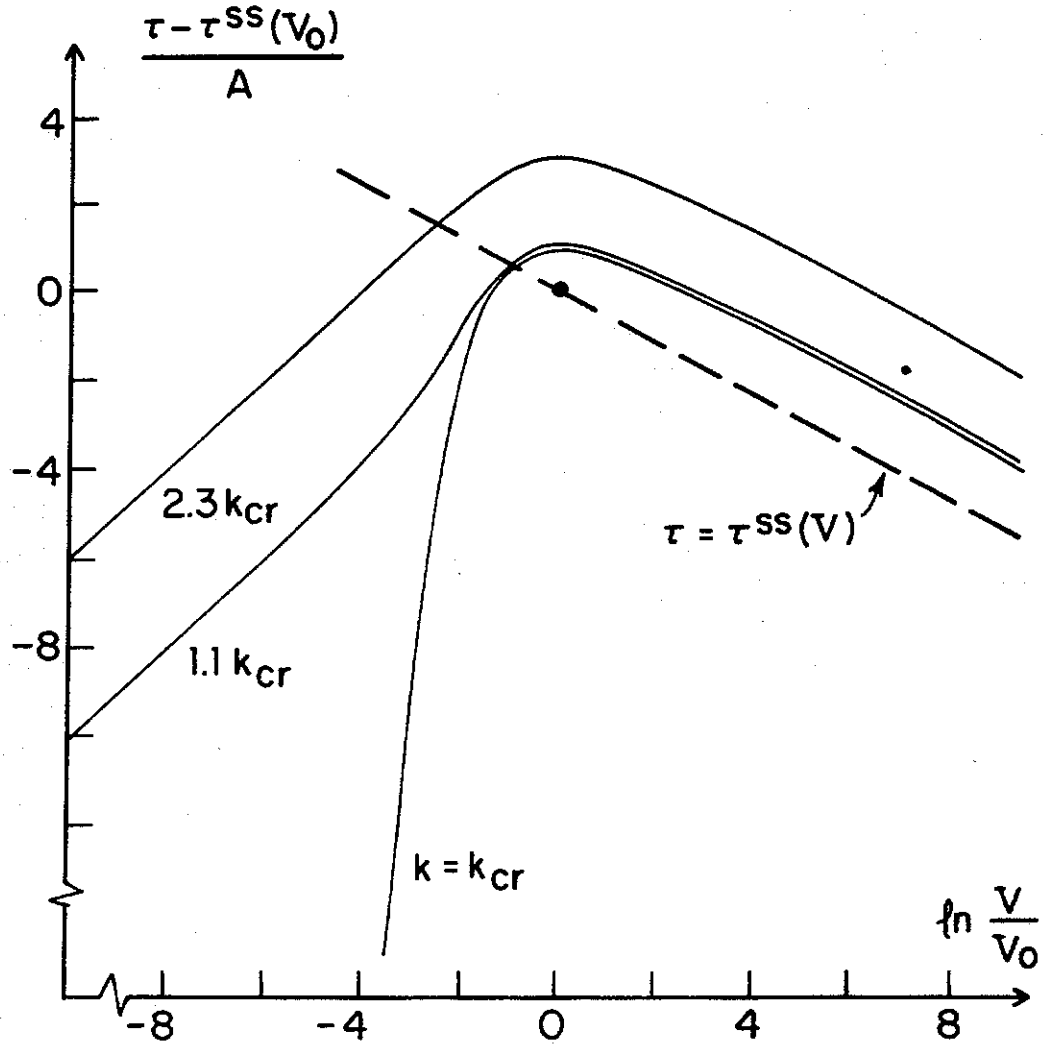

Figure 10. Stability boundaries (after RICE and GU, 1983) corresponding to different stiffnesses for the quasistatic motion of a spring-slider system of stiffness k, with imposed load point motion at constant rate V_0 (i.e., loading rate $\dot{\tau}_0 = kV_0$), based on the one-state-variable constitutive law of equations (29). Drawn for $(B-A)/A = 0.6$, in which case $k_{cr} = 0.6A/L$. The region below each boundary is stable; motions starting there exhibit $V \to V_0$ and $\tau \to \tau^{ss}(V_0)$. Those starting above are unstable, $V \to \infty$ in finte (but sometimes very long) time. Motions starting anywhere are unstable when $k < k_{cr}$; no stability boundary exists in such cases.

with

$$f = (\tau - \tau_*)/A, \quad \lambda = (B-A)/A, \quad K = kL/A. \tag{34}$$

For systems with $B > A$ — i.e., $d\tau^{ss}/dV < 0$ — this family of trajectories has a particular member, given by

$$\tau = \tau_* - (B-A)\ln(V/V_*) + kLB/(B-A), \tag{35}$$

that provides a stability boundary similar to those mentioned earlier (it corresponds to the straight-line limits of the boundaries in Figure 10 for

$V \gg V_0$). All motions beginning at greater values of τ at some given V are unstable in that $V \to \infty$ in finite time. Motions beginning at lesser values of τ are stable, in that $V(t)$ reduces in magnitude toward zero (or, realistically, toward such low values that V_0 can no longer be neglected in comparison to it). By equation (29) this stability boundary for $V_0 = 0$ (or $V \gg V_0$) can be expressed as

$$\tau = \tau^{ss}(V) + kLB/(B - A). \tag{36}$$

As remarked by DMOWSKA and RICE (1984), the same analysis shows that motions beginning in the strip

$$\tau^{ss}(V) + kLB/(B - A) > \tau > \tau^{ss}(V) + kL \tag{37}$$

in the τ-V phase plane are stable in the above sense, but nevertheless show that V initially increases toward a maximum value before beginning monotonic decrease. Motions beginning at values of τ less than the lower limit in (37) show monotonic decrease of V.

Sudden changes in stress on a fault segment, due, say, to a neighboring earthquake, result in suddenly altered values of τ and V. The alterations $\Delta\tau$ and ΔV occur at effectively constant state and thus satisfy (by equation (29))

$$\Delta\tau = A \ln [(V + \Delta V)/V], \tag{38}$$

at least when σ_n is constant, so that A does not change. To the extent that the actual fault segment can be modeled as a single-degree-of-freedom spring–slider, equations (35), (36) give the critical level of the altered stress (to be based on the altered V) that, if exceeded, will lead to an aftershock instability. RICE and GU (1983) use stability boundaries to discuss the effect of this and other types of perturbations on the character of subsequent fault motion.

One of the remarkable features of the constitutive relations discussed is their ability to simulate processes that might be called rehealing or restrengthening. Plainly, the general class of constitutive relations represented by equation (1) allows such phenomena, in that state may alter with time even when $V = 0$. However, the specific constitutive relations given by equations (28), (29), (30) show no change of state when $V = 0$. It is nevertheless the case, as revealed in an insightful analysis of motions based on (29), (30) by RUINA (1980, 1983), that such relations do predict restrengthening in circumstances like those for which it has been observed experimentally. For example, DIETERICH (1972) found that if, after slipping a surface at some rate, the loading ram in his test apparatus was held stationary for some relaxation time t_r before resuming its motion, then the peak stress τ^p encountered in the reinitiation of slip increased with t_r, logarithmically with t_r at large times.

Such experiments can be simulated by the spring–slider system by addressing the following problem: The system slides in steady state with imposed load point speed V_0, and thus exhibits strength $\tau^{ss}(V_0)$. The load point

motion is stopped for some time relaxation time t_r and then resumed again at V_0. What is the peak strength in the subsequent motion? Adopting constitutive relations (29), it is easy to see, following GU *et al.* (1984), that in general some restrengthening must occur, $\tau^p > \tau^{ss}(V_0)$; specific calculations of the effect for different constitutive laws have been reported by DIETERICH (1980), RUINA (1980, 1983) and GU *et al.* (1984). When the load point stops, a relaxation period begins, in which V decreases continuously from V_0 as τ relaxes below $\tau^{ss}(V_0)$; V ultimately attains very low values and the motion may be said to become nearly stationary (the trajectory followed is a member of the family given in equation (33)). During the relaxation Ψ evolves by (29) continuously but incompletely toward values $\Psi^{ss}(V) > \Psi^{ss}(V_0)$. The speed V satisfies $V < V_0$ not only during the relaxation, but also during resumed motion of the load point prior to peak, because $\dot{\tau} = k(V_0 - V) > 0$ prior to peak. It is also seen that $V = V_0$ at peak—i.e., when $\dot{\tau} = 0$. Thus the value Ψ^p at peak exceeds $\Psi^{ss}(V_0)$, and by equations (29) with $V = V_0$ one has

$$\tau^p - \tau^{ss}(V_0) = B[\Psi^p - \Psi^{ss}(V_0)] > 0. \tag{39}$$

This equation confirms the general existence of a restrengthening phenomenon in such circumstances. The specific calculations mentioned above show that $\tau^p - \tau^{ss}(V_0)$ increases with t_r. In fact, RUINA (1983) showed that the peak strengthening predicted from the two-state-variable model of (30), with parameters chosen to fit velocity jump experiments of the type illustrated in Figure 3, gave a close fit to the previous experiments on the same material by DIETERICH (1972) for peak strength as a function of relaxation time. It remains an open question as to whether all low-temeprature restrengthening can be understood as the effect of relaxational slip. The phenomena also may exist on surfaces held in truly stationary contact, as argued by TULLIS and WEEKS (1983) on the basis of recent experiments.

Such restrengthening, whether based on truly stationary contact or on subtle relaxational slip effects, is clearly important to the modeling of repeated earthquakes on the same surface. It allows a repeated sequence of slip-weakening events, except that now the τ versus δ relation followed for each cannot be thought of as universal; rather it has at least some dependence on the elastic stiffness of the fault segment in interaction with its surroundings, as well as on time and rate parameters such as t_r and V_0 in the simple analysis of restrengthening above. The phenomenon allows stress-relieved fault patches to effectively lock, after a previous rapid slip, such that a higher stress than that for rapid slip must be built up to reinitiate slip; the slip, once reinitiated, then continues under decreasing stress, leading to seismic instability in circumstances of sufficiently low stiffness.

DIETERICH (1980) modeled a repeated sequence of such instabilities for a simple spring–slider model, based on his one-state-variable friction law; the analysis bypassed dynamical considerations by artificially imposing a (large) limiting slip velocity on the quasistatic analysis. Recently MAVKO (1984; a

preliminary abstract is given in MAVKO, 1980) has reported a similar analysis for antiplane slip in a continuum fault model of geometry similar to that illustrated in Figure 6a. He uses the constitutive relations of equations (29) and assumes a transition with depth, discontinuous at 15 km depth, between steady-state velocity weakening ($B > A$) in the shallow seismogenic crust and velocity strengthening ($B < A$) at greater depths; A is taken to increase linearly with depth (normal stress dependence). This work appears to be the first nonlinear analysis based on rate-dependent and state-dependent constitutive models for slip between deformable elastic continua. The analysis predicts that the shallow crust remains effectively locked during much of the earthquake cycle, and that it is stressed and driven to instability by a combination of distantly applied loading and local crack-like stress concentration due to slip on the downdip extension of the locked region. Once the upper portion of the crust ruptures, the stress transferred to the essentially stable fault depths below causes a transiently accelerated by aseismic slip there, much as discussed earlier.

Stress and slip distributions appropriate to nonuniform slip on a fault as a slipping zone advances into a locked zone have been shown in Figure 5 and addressed within a rate-independent slip-weakening framework. As mentioned in the associated discussion, such a nonuniform slip rupture mode can be duplicated in the laboratory only in sufficiently large faulted specimens. Recent experiments on a large saw-cut block of granite (DIETERICH, 1980; OKUBO and DIETERICH, 1981; LOCKNER *et al.*, 1982) have produced confined slip events that spread dynamically over the fault (saw-cut) surface during a stick-slip instability. These surfaces are similar to those that comply with rate- and state-dependent friction laws in other laboratory friction tests. When strain-gauge-based measurements of shear stress in adjacent rock are cross-plotted with direct measurements of slip on the fault as the dynamic slip events propagates by a measurement station, there results a τ versus δ relation similar in form to that sketched in Figure 5. Thus the experiments show that a slip-weakening-like response results during dynamic rupture. Recent integrations of equations (29) by GU (private communication, 1983) for rapidly accelerated fault slip confirm that such slip-weakening τ versus δ dependence is consistent with the constitutive description, as already hinted by response to abrupt changes in slip rate like that suggested by Figure 3.

A problem that is still not addressed is whether, in the case of small zones ω of strength degradation, there is any simple generalization of elastic crack mechanics for ruptures on surfaces that follow the rate-and state-dependent constitutive laws. Recall that for the rate-independent case the fault can be analyzed as if it sustains the residual strength τ^f everywhere on slipping regions, resulting in an elastic stress singularity at the advancing tip. The critical intensity factor for the singularity, equation (12), is chosen as to generate the fracture energy identified in Figure 5 and equations (13, 14). A possible generalization to the present context is that one should regard

the slipping part of the fault as sustaining everywhere the steady-state strength $\tau^{ss}(V)$ associated with the local slip rate V. This will be close to correct at positions well removed from the advancing fault tip. There the slip velocities may be presumed to be relatively large and to change slowly enough with time as to undergo little fractional change in slip over distances L; it is straightforward to show that in such circumstances (29) reduces to $\tau = \tau^{ss}(V)$. The same reduction will not be valid near the tip of the slipping region, just as $\tau = \tau^f$ is invalid for the rate-independent case. Possibly, the near tip differences between τ and $\tau^{ss}(V)$ can likewise be lumped into a critical fracture energy G. Now G will also be dependent on propagation speed, and it is to be supplied by an elastic stress singularity calculated for a crack model with $\tau = \tau^{ss}(V)$ everywhere on the crack surface. Of course, the distribution of V is itself not known a priori and is to be solved as part of the complete analysis. Much remains to be done on this topic.

It is to be expected that comparison of predictions based on slip on a single fault with the information that can be extracted from tectonic earthquakes will lead to scaling problems that are similar to those discussed earlier. In particular, it seems likely that larger values of the slip decay distance L will be necessary than can be justified for slip on a single laboratory fault. MAVKO's (1984) simulations are based on L values of the order 10 cm, whereas laboratory measurements to date have suggested values for single fault surfaces that are less than 100 μm. Thus, while the constitutive relations used in such large tectonic-scale simulations may incorporate an acceptable phenomenology, one has at present no reliable route from laboratory tests to assignment of constitutive parameters like A, B, and L. This remains an important problem for earthquake instability theory.

Acknowledgments

The work was supported by the USGS Earthquake Hazards Reduction Program and the NSF Geophysics Program. This paper is based on a presentation at the Workshop on Instabilities in Continuous Media, Venice, Italy, December 1982. Many of the viewpoints expressed grew out of discussions with R. Dmowska, J-C. Gu, V. C. Li, G. M. Mavko, A. L. Ruina, W. D. Stuart, and S. T. Tse. I am also grateful to J. Boatwright, A. McGarr, and G. M. Mavko for supplying copies of their work prior to publication.

REFERENCES

ANDREWS, D. J. (1976), *Rupture velocity of plane-strain shear cracks*, J. Geophys. Res. *81*, 5679–5687.

BOATWRIGHT, J. (1980), *A spectral theory for circular seismic sources: Simple estimates of source dimensions, dynamic stress drop and radiated seismic energy*, Bull. Seismol. Soc. Am. *70*, 1–27.

BOATWRIGHT, J. (1984a), *The effect of rupture complexity on estimates of source size,* J. Geophys. Res. *89,* 1132–1146.

BOATWRIGHT, J. (1984b), *Seismic estimates of stress release,* J. Geophys. Res. (in press).

BRACE, W. F. (1972), *Laboratory studies of stick-slip and their application to earthquakes,* Tectonophysics *14,* 189–200.

BRACE, W. F., and BYERLEE, J. D. (1970), *California earthquakes: Why only shallow focus?* Science, *168,* 1573–1575.

BURRIDGE, R., CONN, G., and FREUND, L. B. (1979), *The stability of rapid mode II shear crack with finite cohesive traction,* J. Geophys, Res. *84,* 2210–2222.

BYERLEE, J. (1968), *Brittle—ductile transition in rocks,* J. Geophys. Res. *73,* 4741–4750.

DAY, S. M. (1982), *Three-dimensional simulation of spontaneous rupture: The effect of nonuniform prestress,* Bull. Seismol. Soc. Am. *72,* 1881–1902.

DIETERICH, J. H. (1972), *Time-dependent friction in rocks,* J. Geophys. Res. *77,* 3690–3697.

DIETERICH, J. H. (1978), *Time dependent friction and the mechanics of stick slip,* PAGEOPH *116,* 790–806.

DIETERICH, J. H. (1979a), *Modeling of rock friction 1: Experimental results and constitutive equations,* J. Geophys. Res. *84,* 2161–2168.

DIETERICH, J. H. (1979b), *Modeling of rock friction 2: Simulation of preseismic slip,* J. Geophys, Res. *84,* 2169–2175.

DIETERICH, J. H., *Experimental and model study of fault constitutive properties,* in *Solid Earth Geophysics and Geotechnology* (ed. S. Nemat–Nasser) (Appl. Mech. Div., vol. 42, Am. Soc. Mech. Eng., NY 1980), pp. 21–30.

DIETERICH, J. H., *Constitutive properties of faults with simulated gouge,* In *Mechanical Behavior of Crustal Rocks* (eds. Carter, N. L., Friedman., M., Logan, J. M., and Stearns, D. W.) (Geophys. Monogr. Ser. No. 24, Am. Geophys. Union, Washington, D.C. 1981) pp. 103–120.

DMOWSKA, R., and LI, V. C. (1982), *A mechanical model of precursory source processes for some large earthquakes,* Geophys. Res. Lett. *9,* 393–396.

DMOWSKA, R., and RICE, J. R., *Fracture theory and its seismological applications,* in *Continuum Theories in Solid Earth Physics* (ed. Teisseyre, R.) (Elsevier, Amsterdam, in press, 1984).

GU, J.-C., RICE, J. R., RUINA, A. L., and TSE, S. T. (1984), *Slip motion and stability of a single degree of freedom elastic system with rate and state dependent friction,* J. Mech. Phys. Solids *32* (3).

HIGGS, N. G., *Mechanical properties of Ultrafine Quartz, Chlorite and Bentonite in environments appropriate to upper-crustal earthquakes* (Ph. D. Thesis, Texas A and M University, August 1981).

IDA, Y. (1972), *Cohesive force across the tip of a longitudinal shear crack and Griffith's specific surface energy,* J. Geophys. Res. *77,* 3796–3805.

IDA, Y. (1973), *The maximum acceleration of seismic ground motion,* Bull. Seismol. Soc. Am. *63,* 959–968.

LI, V. C., and RICE, J. R. (1983a), *Preseismic rupture progression and great earthquke instabilities at place boundaries,* J. Geophys. Res. *88,* 4231–4246.

LI, V. C., andRICE, J. R. (1983b), *Precursory surface deformation in great plate boundary earthquake sequences,* Bull. Seismol. Soc. Am. *73,* 1415–1434.

LOCKNER, D. A., OKUBO, P. G., and DIETERICH, J. H. (1982), *Containment of stick-slip failures on a simulated fault by pore fluid injection,* Geophys. Res. Lett. *9,* 801–804.

MAVKO, G. M. (1980), *Simulation of creep events and earthquakes on a spatially variable model* (abstr), EOS, Trans. Am. Geophys. Union *61,* 1120.

MAVKO, G. M. (1984), *Large-scale earthquakes from a laboratory friction law,* J. Geophys. Res. (in press).

MCGARR, A. (1984), *Scaling of ground motion parameters, state of stress and focal depth,* J. Geophys. Res. (in press).

OKUBO, P. G., and DIETERICH, J. H. (1981), *Fracture energy of stick-slip events in a large scale biaxal experiment*, Geophys, Res. Lett. *8*, 887–890.

PALMER, A. C., and RICE, J. R. (1973), *The growth of slip surfaces in the progressive failure of overconsolidated clay slopes*, Proc. R. Soc. Lond., *A332*, 527.

RABINOWICZ, E. (1958), *The intrinsic variables affecting the stick slip process*, Proc. Phys. Soc. *71*, 665–675.

RICE, J. R., *The mechanics of earthquake rupture*, In *Physics of the Earth's Interior* (Proceedings of the International School of Physics 'Enrico Fermi', Course 78, 1979) (ed. Dziewonski, A. M., and Boschi, E.) (Italian Physical Society, printed by North Holland, Amsterdam 1980) pp. 555–649.

RICE, J. R., *Shear instability in relation to the constitutive description of fault slip*, in *Rockbursts and Seismicity in Mines* (eds. Gay, N. C. and E. H. Wainwright) (Symp. Ser. No. 6, South African Institute of Mining and Metallurgy, Johannesburg, 1984), pp. 57–62.

RICE, J. R., and GU, J.-C. (1983), *Earthquake aftereffects and triggered seismic phenomena*, Pure Appl. Geophys. *121* (2).

RICE, J. R., and RUINA, A. L. (1983), *Stability of steady frictional slipping*, Trans. ASME, J. Appl. Mech. *50*, 343–349.

RUDNICKI, J. W. (1980), *Fracture mechanics applied to the earth's crust*, Annu. Rev. Earth Planet. Sci. *8*, 489–525.

RUINA, A. L., *Friction Laws and Instabilities: A Quasistatic Analysis of Some Dry Frictional Behavior* (Brown University, Ph. D. Thesis, 1980).

RUINA, A. L. (1983), *Slip instability and state variable friction laws*, J. Geophys. Res. (in press).

STESKY, R. M. (1978), *Mechanisms of high temperature frictional sliding in Westerly granite*, Can. J. Earth Sci. *15*, 361–375.

STUART, W. D. (1979a), *Strain softening prior to two-dimensional strike slip earthquakes*, J. Geophys. Res. *84*, 1063–1070.

STUART, W. D. (1979b), *Strain-softening instability model for the San Fernando earthquake*, Science *203*, 907–910.

STUART, W. D., and MAVKO, G. M. (1979), *Earthquake instability on a strike-slip fault*, J. Geophys, Res. *84*, 2153–2160.

TULLIS, T. E., and J. D. WEEKS, (1983), *Increase in frictional strength of granite during static contact* (abstr), EOS, Trans. Am. Geophys. Union *64*, 317.

WONG, T.-F. (1982), *Shear fracture energy of Westerly granite from post-failure behavior*, J. Geophys. Res. *87*, 990–1000.

(Received November 1983, revised December 1983, accepted January 1984)